ERNEST ORLANDO LAWRENCE BERKELEY NATIONAL LABORATORY

Measurement of Passive Uptake Rates for Volatile Organic Compounds on Commercial Thermal Desorption Tubes and the Effect of Ozone on Sampling

Randy Maddalena[1], Amanda Parra[1,2], Marion Russell[1], Wen-Yee Lee[1,2]

[1]Environmental Energy Technologies Division
 Energy Analysis and Environmental Impacts Department
Lawrence Berkeley National Laboratory
Berkeley, CA 94720

[2]Chemistry Department
University of Texas at El Paso
El Paso, TX 79968

May 2013

DISCLAIMER

ACKNOWLEDGMENTS

Table of Contents

ABSTRACT

Diffusive or passive sampling methods using commercially filled axial-sampling thermal desorption tubes are widely used for measuring volatile organic compounds (VOCs) in air. The passive sampling method provides a robust, cost effective way to measure air quality with time-averaged concentrations spanning up to a week or more. Sampling rates for VOCs can be calculated using tube geometry and Fick's Law for ideal diffusion behavior or measured experimentally. There is evidence that uptake rates deviate from ideal and may not be constant over time. Therefore, experimentally measured sampling rates are preferred. In this project, a calibration chamber with a continuous stirred tank reactor design and constant VOC source was combined with active sampling to generate a controlled dynamic calibration environment for passive samplers. The chamber air was augmented with a continuous source of 45 VOCs ranging from pentane to diethyl phthalate representing a variety of chemical classes and physiochemical properties. Both passive and active samples were collected on commercially filled Tenax TA thermal desorption tubes over an 11-day period and used to calculate passive sampling rates. A second experiment was designed to determine the impact of ozone on passive sampling by using the calibration chamber to passively load five terpenes on a set of Tenax tubes and then exposing the tubes to different ozone environments with and without ozone scrubbers attached to the tube inlet. During the sampling rate experiment, the measured diffusive uptake was constant for up to seven days for most of the VOCs tested but deviated from linearity for some of the more volatile compounds between seven and eleven days. In the ozone experiment, both exposed and unexposed tubes showed a similar decline in terpene mass over time indicating back diffusion when uncapped tubes were transferred to a clean environment but there was no indication of significant loss by ozone reaction.

KEYWORDS

Indoor Air Quality, VOCs, Passive Sampling, Uptake Rates

INTRODUCTION

Individuals spend the majority of their time indoors. On average, people spend 87% of their time either indoors at home or in office buildings and 6% of their time in vehicles (Klepeis et.al. 2001). A wide variety of volatile organic compounds (VOCs) and other air pollutants (such as ozone, carbon monoxide, carbon dioxide, nitrogen dioxide and particulate matter) can impact indoor air quality (Maddalena et.al. 2012; Hodgson and Levin, 2003), occupant health (Logue et.al. 2011) and performance (Satish et.al. 2011). The indoor air concentration of VOCs in particular often exceeds concentrations typically found in outdoor air. This is due, in part, to the presence of chemical sources in residential, public and commercial buildings including: building materials, consumer products, cleaning products, pesticides, and activities such as smoking, printing, cleaning and cooking. Indoor air concentrations of VOCs are influenced by fresh air ventilation rates in buildings where the combination of chemical sources and low ventilation rates can result in elevated exposures for building occupants. Exposure to high levels of VOCs has been linked to a variety of adverse health effects ranging from cancer to sensory irritation. Measuring the levels of VOCs present in indoor air is therefore an important component of indoor air quality assessment.

Actively collecting air samples onto adsorbent media is a well-established technique that has been widely used for indoor air quality assessments. The approach uses a calibrated pump to pull a known volume of air through sorbent material over a predetermined time interval or integration period (Woolfenden & McClenny, 1999). Chemicals are trapped on the sorbent to be later desorbed for measurement, typically by thermal desorption and gas chromatography/mass spectrometry (TD-GC/MS). The TD-GC/MS analysis determines the mass of each target chemical on the sorbent and then the average concentration over the sampling period is determined by dividing the mass by the total volume of air sampled. The integration period for active sampling is relatively short with typical sampling periods from 30 minutes to several hours. The lower limit on integration period is dictated by the maximum face velocity of air that can be sustained without chemical break through (ASTM D 6196-03). The upper limit on integration period is determined by the minimum flow rate that can be sustained using a pump without molecular back-diffusion biasing the results. Although active sampling techniques are well established and highly reliable, the approach has several disadvantages. For example, active sampling typically requires either trained personnel or expensive control systems, and uses pumps that are heavy, noisy and not easily adaptable to either ultra-slow or intermittent sampling. As a result, active sampling methods are not well suited for long-term integrated sampling, for deployment by un-trained personnel (i.e. home owners or building managers), or for large scale sampling events requiring multiple co-deployed samplers to improve spatial resolution.

Passive sampling techniques are also well established (ASTM D 6196-03) and widely used (Jia et.al. 2011; Walgraeve et.al. 2011). The samplers work continuously by molecular diffusion through a fixed boundary layer once the sampling device is opened to the environment. Passive sampling rates are controlled by the chemical's molecular diffusivity (D_{air}, cm^2/min), the projected surface area of the sorbent face (A, cm^2) and the diffusion path length (L, cm). The integration period (length of sampling time) is limited only by the sorbent capacity or the sorbent/air partition coefficient ($K_{s/a}$, unitless).

There are three types of commercially available passive VOC samplers. Badge samplers can be worn for personal monitoring but require special extraction procedures to analyze. Radial diffusive samplers collect through the walls of a tube providing larger sorbent surface area (and sampling rate) and are processed either by solvent extraction or thermal desorption.

Axial diffusive samplers are based on the design of standard thermal desorption tubes collecting sample through an open end of the tube and are processed in the same manner as active samples by thermal desorption. The axial diffusion sampling tubes are most convenient because they utilize the same sampling tubes and analytical methods as active sampling but allow for much longer integration periods. These longer integration periods can better reflect chronic exposure for building occupants or workers. Passive sampling techniques are quiet, simple, require no power or extra equipment and may be deployed by anyone following simple written instructions. These attributes allow a researcher to do large-scale or field studies more easily than with active sampling.

Unlike active sampling techniques where the sampling rate is controlled by a pump and is the same for all chemicals in the sample, passive sampling rates depend on molecular diffusivity, sampler geometry and sorbent capacity so chemical and sampler specific sampling rates need to be used. Sampling rates or uptake rates (UR, mL/min) can be calculated for diffusive samplers from Fick's Law as

$$UR = \frac{D_{air} \times A}{L} \qquad (1)$$

Where D_{air} (cm^2/min) is the chemical specific molecular diffusivity, A (cm^2) is the projected surface area of the sorbent face or cross sectional area of the tube opening in the axial sampler, and L (cm) is the diffusion path length or distance from the entrance of the tube to the face of the sorbent material. Most commercially available thermal desorption tubes are built to tight specifications with the distance from opening to face of sorbent set to 15 mm.

Actual uptake rates often deviates from the theoretical uptake rate represented by Equation 1 (Walgraeve et.al. 2011a and 2011b; Gonzalez-Flesca and Frezier, 2005; Yılmaz Civan et.al. 2012; ASTM D 6196-03; Kumar and Viden, 2007) so it is necessary to experimentally determine uptake rates under application relevant conditions.

Uptake rates can be determined experimentally with either field measurements or chamber measurements. In both cases the uptake rate is measured by co-locating active and passive samplers then calculating uptake volume (V, Liters) using the blank corrected mass on the passive sampling tube and the time-averaged concentration determined with the active sampler. Then uptake rate (UR) is determined dividing V by the duration of sampling event as shown in Equation 2.

$$UR = \frac{(m - m_b)}{C} \times t^{-1} \qquad (2)$$

Where m is the mass measured in the diffusion tube (μg), m_b is the mass of chemical measured in a blank tube that is co-deployed with the diffusive sampler but remains capped during the sampling period, C (μg/L) is the time averaged concentration measured by active sampling over the period of diffusive uptake and t (min) is the duration of the diffusive uptake period.

There are a number of different commercially available thermal desorption tubes that can be used as axial-diffusive passive samplers. Tubes from different manufacturers may vary in internal diameter, overall length and material but a common diffusion path length (distance from tube opening to face of sorbent) is typically used. Press-on diffusion caps with metal gauze across the opening are typically used on the inlet side of an axial-diffusion tube during

sampling to mitigate effects of wind on diffusive uptake rate while the outlet side of the tube remains closed.

Similar to active sampling tubes where the sorbent material is selected to provide sufficient capacity to limit chemical breakthrough during sampling, the capacity of the sorbent material used in passive sampling tubes is selected to prevent back diffusion of target compounds (Brown and Shirly, 2001; ASTM D 6196-03). However, there is evidence that ozone reactions may consume VOCs sorbed to surfaces (Springs et.al. 2011; Coleman et.al. 2008). Ozone reaction with sorbed VOCs may lead to losses of chemical mass during the sampling period. If ozone reactions are found to bias diffusive sampling results, it may be necessary to use ozone scrubbers on the inlet to the axial-diffusive sampling tubes. Although it is commonly recommended that ozone scrubbers be used for aldehyde sampling, no information is available to determine if ozone scrubbers are needed for passive VOC sampling.

The aims of this study were to 1) experimentally determine the passive sampling uptake rates for a broad range of indoor relevant VOCs using commercially available sampling tubes, 2) explore the effects of ozone on the stability of terpenes sorbed passively to axial diffusion tubes, and 3) provide recommendations for passive sampling of VOCs in indoor air quality assessments.

METHODS

Overview
A list of target compounds representing a range of chemical classes and physiochemical properties was identified from previous indoor air quality studies. These compounds were mixed at equal mass in a solution and injected at a constant rate into a heated glass tube where the mix was rapidly volatilized and swept into a continuous stirred tank reactor chamber producing a controlled well-mixed atmosphere at ambient temperature and humidity. Pre-conditioned axial diffusion tubes with diffusion caps were installed at different orientations in the chamber at the start of the sampling period. Two tubes were harvested each day over a period of eleven days for passive uptake determination. Active samples were collected twice daily to measure the time-averaged concentration of each target chemical. The results were used to calculate sampling rates for the target compounds.

A second experiment was conducted to test ozone interaction with sorbed VOC. The chamber was spiked with a continuous mix of terpenes over seven days. Passive samplers were deployed without diffusion caps at the start of the sampling period. Both passive and active samples were collected daily and used to estimate uptake rates. At the end of seven days, the remaining twelve sampling tubes were removed from the chamber. The terpene delivery system was removed and an ozone generator installed. Once ozone levels in the chamber stabilized at the target level, nine tubes were configured with either a potassium iodide (KI) coated denuder (ozone scrubber), an uncoated denuder, or left with an open inlet and returned to the chamber with elevated ozone. The remaining three tubes were placed in an ozone free environment with an unmodified open inlet. After four days, all tubes were harvested and analyzed to determine the effect of ozone exposure on sorbed VOCs.

Details of the experiments are provided below.

Reagents
Pure chemicals ($\geq$ 98% purity) were used in this study (Sigma-Aldrich, Fluka). Two VOC mixtures were prepared by mixing equal amounts (by mass) of each target compound listed in

Appendix 1 found at the end of this document. Chemicals are sorted by compound class and increasing boiling point. Target compounds were selected to represent a wide range of indoor pollutants with different physiochemical properties that are relevant to indoor air quality assessments. The first mix includes all the compounds in Appendix 1 and was used for the diffusive uptake measurements while the second chemical mix was prepared with just the terpenes: 3-carene, α-pinene, γ-terpiene, α-terpineol and d-limonene and used for the ozone experiment. The relevant physiochemical properties for each compound are provided in Appendix 1.

The property values in Appendix 1 were either taken from the original container of the pure compound or looked up on-line at ChemSpider.com where the molecular weight (*MW*, g/mol) and CAS number are reported under chemical identification; boiling point (*BP*, °C) is from the experimental database; molar volume (V_x, cm^3/mol) is from the Predicted-ACL/Labs tab and the remaining properties are from the Predicted-EPISuite tab. Diffusivity in air (D_{air}, cm^2/s) is calculated (Tucker and Nelken, 1990) as

$$D_{air} = 9.95 \times 10^{-4} T^{1.75} \frac{\sqrt{\frac{(29+MW)}{29MW}}}{\left[2.7+(V_x)^{1/3}\right]^2} \tag{3}$$

Where *T* is the air temperature (kelvin), *MW* is the molecular weight of compound of interest (g/mol), and V_x is the molecular volume of the compound (cm^3/mol). The values 29 and 2.7 represent the molecular weight and cubic root of molecular volume, respectively, for air.

Ozone scrubber preparation
Ozone scrubbers were prepared using a potassium iodide solution by mixing equal parts of (A) a 20 g of KI (> 99%, Aldrich) in 10 mL of de-ionized water, and (B) 10% (v:v) glycerol in methanol solution. The mixture was stirred 15 min with no added heat and used to coat the inside of denuder tubes mounted at the inlet of the samplers.

Calibration Chamber
A medium-scale (395 L) continuous stirred cylindrical frame flow through chamber constructed with a Teflon-coated aluminum frame wrapped in a transparent Teflon film shown in Figure 1 was used for the uptake experiments. The continuous stirred tank reactor (CSTR) design was originally used in chemical engineering applications but later adapted for use with biological systems (Jeffries et.al., 1976) and for investigating the interaction between trace pollutants and plants (Rogers et.al., 1977; Heck et.al., 1978). The design has since been used to measure uptake of semi-volatile organic compounds into vegetation (Maddalena et.al. 2002) and to measure active emission rates from computers and printing devices (Maddalena et.al. 2010). The CSTR design provides near ideal mixing so that test compounds introduced in the inlet of the exposure chamber are uniformly mixed throughout the system. As a result, measurements collected at the chamber exit port are representative of the concentration at any point within the chamber (Heck et.al., 1978). By constructing the CSTR from Teflon coated material and film, the interaction of pollutants with the chamber walls is minimized providing an ideal environment for calibration of passive sampling uptake rates.
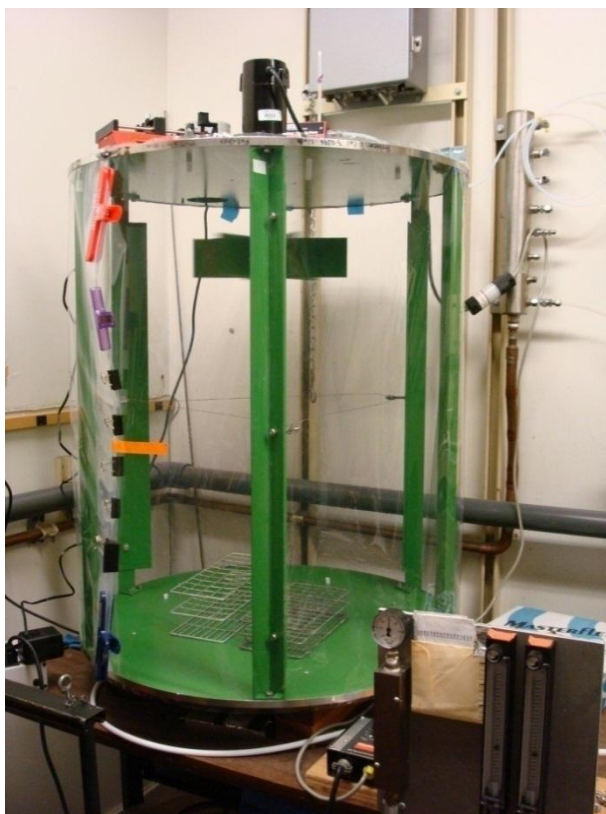
Figure 1. Medium scale Teflon Continuous Stir Tank Reactor chamber. Photo shows the chamber setup for measuring passive sampling rates in commercially filled Tenax TA thermal desorption tubes.

Room air is drawn into the CSTR through a bed of activated carbon (Purafil® SP media) to remove background contaminants. The chamber temperature and relative humidity (*RH*) were controlled by conditions in the room ($T = 22.5 \pm 0.5$ ˚C and $RH = 35\% \pm 5\%$). Environmental variables (*T*, *RH* and pressure differential [inside-outside]) are logged continuously during operation (HOBO model U10 Temp/RH Data Logger). The chamber is equipped with a controlled CO_2 source and continuous CO_2 analyzer for air exchange rate confirmation as needed. Air change rate during the study was maintained at 2.0 ± 0.2 per hour during the diffusive sampling experiment and 1.0 ± 0.2 per hour during the ozone experiment. Chamber exhaust was evacuated to a fume hood using a continuous flow rotary vane pump and rotometer flow control valves. An impellor mounted at the top of the chamber and operated at approximately 50% power insures homogeneous mixing in the chamber.

The VOC mixtures were introduced into the chamber using a programmable syringe pump (NE-4000; New Era Pump Systems), fitted with a 500 mL glass syringe. The syringe was connected to a Tube Spiking Apparatus (TSA, Gerstel US) set at 100 ˚C for the VOC uptake experiment and 40 ˚C for loading terpenes during the ozone experiment. The VOC mixture was introduced at a rate of 0.03 µL/min for the VOC uptake experiment and 0.013 µL/min for the ozone experiment. The mixture was volatilized in the TSA and swept into the chamber with a continuous flow of house air (500 mL/min).

Ozone was generated by passing house air through a glass tube exposed to UV light in a Stable Ozone Generator (model 50G-2). An O_3 analyzer (Advanced Pollution Instrumentation, model 400) was used to monitor the ozone levels in the chamber. Ozone was added to the chamber at a constant rate through a Teflon tube inserted into the inlet air stream

providing a steady-state ozone concentration between 10 and 20 ppb, which is a representative range for what might be found in indoor environments.

Passive Sampling

The original study design included two different axial-diffusive samplers (Gerstel and PerkinElmer) but only the Gerstel tubes were analyzed.

The diffusive uptake experiment used stainless steel Tenax®-TA sorbent tubes with an inner diameter of 4 mm, outside diameter of 6 mm, and 17.8 cm length (Supelco, 28271-U). Tubes were pre-conditioned in a tube conditioning unit (TCU, Gerstel US) with high purity helium at 40 mL/min and 315 ˚C for 1 hour. After the CSTR concentrations reached steady-state, the tubes were deployed in the chamber at different orientations with the front end of the tubes fitted with standard diffusion caps (Supelco, 28017-U) and the outlet from the tube capped with a swage cap and Teflon ferrule. Two tubes were harvested every 24 hours during the uptake period, transferred to storage sleeves with Teflon lined caps (Supelco, 25095-U) and stored at -20 ˚C until analysis.

The ozone experiment used stainless steel Tenax®-GR sorbent tubes with an inner diameter of 4 mm, outside diameter of 6 mm, and 17.8 cm long (Supelco, 28272-U). Tubes were pre-conditioned in a tube conditioning unit (TCU, Gerstel US) with high purity helium at 40 mL/min and 315 ˚C for 1 hour. Diffusion caps were not used for the ozone experiment because the original purpose was only to passively load terpenes on tubes for subsequent ozone exposure. After the CSTR concentrations reached steady-state with the terpene mix, the tubes were deployed in the chamber at different orientations with the front end of the tube open to the environment and the back end of the tube capped with a swage fitting and Teflon ferrule. Two tubes were harvested every 24 hours during the uptake period, transferred to storage sleeves with Teflon lined caps (Supelco, 25095-U) and stored at -20 ˚C until analysis. At the end of the uptake period, the remaining tubes were collected and capped then used in the ozone exposure experiment described later.

Active Sampling

Active VOC samples were collected on multibed sorbent tubes (Gerstel, P/N 012347-005-0) with a primary bed of Tenax-TA® (2/3 by volume) and a smaller secondary bed of Carbosieve® (1/3 by volume). These tubes had the same dimensions as the passive sorbent tubes described above and were conditioned as described above. VOC samples were collected directly onto the sorbent tubes from a port in the chamber top. A variable speed peristaltic pump (Cole-Parmer Instrument Company, Model 7553-80) was used to pull air from the chamber at a flow rate of 60-65 mL/min for 30 min (Approximately 2 liters were collected for each sample). Flow rates were measured twice during the sampling period using a DryCal gas flow meter (BIOS, 500 cc/min) at the exit from the pump. Active sampling was typically conducted twice each day (morning and afternoon). After sampling, the tubes were transferred to storage sleeves with Teflon lined caps (Supelco, 25095-U) and stored at -20 ˚C until analysis. Analysis was typically completed within 4 days of sample collection.

Test for Ozone Interference on Axial-Diffusion Samplers

Several papers have shown that ozone can react with terpenes on Tenax sorbent during active sampling (Calogirou et al. 1996; Pollmann et al. 2005). Research with aldehyde sampling in the presence of ozone found that potassium iodide is the most effective scrubber for removing ozone upstream of air sampling devices (Kleindienst et al, 1998). To test the need for ozone scrubbing during passive sampling, we developed a potassium iodide (KI) coated denuder extension that is connected to the sampling end of the axial-diffusion tube.

The KI coated denuders were prepared by cutting 3 cm length sections of ¼ inch stainless steel tubing. Tube sections were cleaned by sonication in methanol for 15 min followed by baking in an oven for 20 min at 60C°. Equal parts of the KI solution and glycerol solution (see Reagents above) was transferred into the denuders and allowed to set for 7 minutes to allow KI to sorb onto the inner wall of the tube sections. The solution was then drained, and the denuder was air-dried on a solid phase extraction manifold under slight vacuum for 20 min. The preparation resulted in ~ 20 mg KI coated onto each denuder section. The sections were connected to the inlet of the axial diffusion tube using press fittings (McMasterCarr, p/n 51495K413). Three configurations were used during the ozone exposure – denuder with KI coating, denuder without KI coating, and no denuder. The "no denuder" configuration was included in both the ozone exposure and ozone free environment.

To test for ozone interaction, a set of five mono-terpenes were passively loaded on axial-diffusion tubes as described above under the "passive sampling" section. After completion of terpene loading period, the remaining 12 sampling tubes were removed from the chamber and capped for later use. The VOC source was removed from the CSTR and the chamber was purged with clean air until active sampling confirmed the absence of terpenes. Once all terpenes were flushed from the CSTR, an ozone generator was installed on the chamber and adjusted to a chamber concentration of 10-20 ppb ozone at steady state.

Once the ozone level was stabilized, four treatments were initiated: (i) three tubes without denuder sections were exposed in a second stainless steel ozone free chamber running at 2.5 air changes per hour; (ii) three tubes without denuders sections installed in the CSTR with ozone; (iii) three tubes with denuder sections that were not coated with KI in the CSTR; and (iv) three tubes with KI coated denuders sections in the CSTR. All samples were exposed for four days (3 in the ozone free chamber and 9 in the ozone spiked CSTR) and analyzed for VOC at the end of the exposure period.

Chemical Analysis

The sorbent tubes were spiked with internal standard (~120 ng 1-bromo-4-fluorobenzene) and purged in the direction of sampling at room temperature for 3 minutes (40 mL/min) prior to analysis. The purging was used to ensure that the ISTD was transferred to the sorbent. Tubes were thermally desorbed for analysis by gas chromatography/mass spectrometry (TD-GC/MS) using a thermodesorption auto-sampler (Model TDSA2; Gerstel), a thermodesorption oven (Model TDS3, Gerstel) and a cooled injection system (Model CIS4; Gerstel). The cooled injection system was fitted with a Tenax-packed glass liner (P/N 013247- 005-00; Gerstel). Desorption temperature was 25 ℃ with a 0.5 minute delay followed by a 60 ℃/min ramp to 270 ℃ and a 4 minute hold time. The cooled inlet was held at -10 ℃ and then heated within 0.2 minutes to 270 ℃ at a rate of 12 ℃/s, followed by a 3-minute hold time. Compounds were resolved on a GC (Series 6890Plus; Agilent Technologies) equipped with a 30 meter HP-1701 14% Cyanopropyl Phenyl Methyl column (Model 19091U-233; Agilent Technologies) at an initial temperature of 1 ℃ for 0.5 minutes then ramped to 40 ℃ at 25 ℃/min, to 115 ℃ at 3 ℃/min and finally to 250 ℃ at 10 ℃/min holding for 10 minutes. Column flow was constant at 1.2 mL/min. The resolved analytes were detected using a mass spectrometer (5973; Agilent Technologies). The MS was operated in scan mode. Multipoint calibrations were prepared from pure standards for all target VOCs. All analytes were referenced to the internal standard.

Data Analysis

The chemical specific theoretical uptake rate (*UR,* mL/min) is calculated from Fick's Law shown in Equation 1 of the introduction where the cross sectional area (*A,* cm^2) of the axial

diffusion tubes (not corrected for gauze diffusion cap) used in this work is 0.1257 cm^2 and the diffusion path length is 15 mm.

The experimental uptake rate was calculated from Equation 2 in the introduction where the blank corrected chemical specific mass was measured on the passive sampling tubes for each time point (two samplers per day) and the time averaged exposure concentration was from active samples collected daily during the exposure period. Because the passive sampling period or end-point did not always coincide with the active sample collection, the concentrations used with Equation 2 were interpolated between the two closest time-averaged concentrations to coincide with the actual end time of the passive sample.

The experimental uptake rate (mL/min) for each chemical was plotted as a function of time (days) to determine if the rate was constant (linear) or if the sorbent capacity was reached (deviation from linearity) and a regression model fit to the data using Excel (Microsoft Office 2010).

Measured uptake rates were compared to published values. Some published uptake rates are reported in units of ng/ppm (V/V)/min identified in this report as UR_m. The uptake rates are converted to the volumetric uptake rate (UR, mL/min) by

$$UR = UR_m \times \frac{24.45}{MW} \times \frac{101}{P} \times \frac{T}{298} \tag{4}$$

Where P (kPa) is the actual pressure of the air sampled and T (kelvin) is the absolute temperature of air during sampling. It follows that if atmospheric pressure and temperature deviate significantly from standard temperature and pressure then the uptake rate for a given T and P (UR') is calculated by

$$UR' = UR \times \frac{101}{P} \times \frac{T}{298} \tag{5}$$

For the ozone experiment, the four treatments were compared to each other and to the final mass measured at the termination of the uptake experiment. The objective was to quantify the change in terpene mass on the tubes caused by exposure of the sorbed compounds to ozone. The data also provide a measure of the effect of the diffusion end caps on uptake rates and an estimate of diffusive loss during storage for un-capped tubes. Student's t-test was used along with an estimate of percent difference (*%Diff*) between each treatment where *%Diff* is

$$\%Diff = \frac{(Value_1 - Value_2)}{average(Value_1, Value_2)} \times 100 \tag{6}$$

RESULTS

Experimental conditions and active sample concentrations

The uptake experiment started with forty-four chemicals listed in Appendix 1 and mixed at an equal mass concentration except for compounds with boiling points greater than 220 ºC, which were added at half the concentration compared to the others. Several days of testing were required in the chamber to identify the conditions needed to produce a steady state concentration in the range of 30 to 50 µg/m^3. The measured concentrations from active sampling are presented in the first column of plots in Figure 2. These values represent the actual concentration in the chamber at the time of sampling integrated over the ~ 30 minute period of active sampling. As a result, the raw data represent a series of snap shots or short

term measurements collected over the duration of the study. The raw data were used to calculate the time averaged concentration and the results are shown in the second column of plots in Figure 2. The time averaged concentration represents the integrated concentration over the experimental period.

The zero time point was collected immediately following loading of the passive sampling tubes into the CSTR and typically shows a lower concentration caused by ventilation of the chamber during loading. The concentration in the chamber with a constant source and ventilation rate of 2.0 air changes per hour (ACH, h^{-1}) is expected to reach steady state within about 3/ACH hours or 1.5 hours. The concentration trend lines for most of the compounds achieved steady-state by the first sampling point, approximately 16 hours after loading the tubes.

Three chemicals did not behave as expected during the uptake experiment. Dichloromethane (DCM) and hexane each had two high concentration spikes early in the exposure period with the remainder of measurements in agreement with other compounds. The cause of these spikes was unknown but DCM and hexane are commonly used solvents in the laboratory so the spikes may have been due to elevated background from other lab activity. Dibutylphthalate concentration came up very slowly and then the concentration dropped below the limit of detection at about 100 hours but increased again through the end of the experiment. This erratic concentration behaviour may have been related to the low volatility of dibutylphthalate causing interactions with the source tubing and the chamber walls or may hav e been due to poor mixing in the VOC source solution.

All of the VOC concentrations in the CSTR began to drop after about 220 hours (day nine) of exposure. This drop occurred over a weekend and was probably caused by a failure or depletion of the VOC source. The time average concentration (column to right of plots in Figure 2) was provided through the entire experimental period (11 days). Uptake rates are calculated for both the constant source period (zero to 220 hours) and the full experimental period.

Volumetric sampling rates for passive sampling

The cumulative air volume sampled (V, Liters) is calculated from the time averaged active sampling concentrations and the mass on the passive sampling tube for each time point. The results are reported for each time point and the individual compounds in each chemical class on the plots to the left of Figure 3. Because the cumulative volumetric uptake was not linear over the entire experiment for all compounds, a power function was used to describe uptake as

$$V = mx^z \tag{7}$$

Where V is the vector of determined cumulative volumetric uptakes (L) and x is vector of elapsed times (h). The constants in Eq. 7 are calculated in Excel$^{®}$ as

$z = \text{SLOPE}(\text{LN}(V),\text{LN}(x))$ (8)

$m = \text{EXP}(\text{INTERCEPT}(\text{LN}(V),\text{LN}(x)))$ (9)

and the coefficient of determination for the curve fit is

$r^2 = \text{RSQ}(\text{LN}(V),\text{LN}(x))$ (10)

The power function is useful for this application because it always intercepts at zero and as the value of z approaches 1, the trend becomes linear. Equations 7-9 are used to calculate the cumulative uptake volume by fitting the measured data from the first nine days of the experiment (steady-state period) and separately by fitting the measured data from the full 11-day experiment. For compounds where the exponent z exceeded 1, a linear regression with zero intercept was used to describe the volumetric uptake. The linear regression resulted in an increased coefficient of determination (r^2). The linear regression was used for seven compounds including 2-butoxy ethanol, texanol, TXIB, dimethyl phthalate, diethyl phthalate, dibutyl phthalate and a-terpineol.

The curves of cumulative sample volume versus time for many of the compounds show a pattern with an initial uptake rate that is faster than the long-term average. A decreasing sampling rate over time is consistent with other studies using Tenax axial-diffusive sampling tubes (Walgraeve et.al., 2011; Civan et.al., 2012) and is thought to be related to the capacity of the sorbent for the compound (Pennequin-Cardinal et.al., 2005). Replicate measurements were collected at each time point and the replicates demonstrate very good precision in the data used for the regression analysis. This provides a high degree of confidence in the shape of the uptake curves.

The fitted parameters from the regression analysis were used to estimate cumulative sample volume which was then used with Equation 2 to estimate the time averaged uptake rate for each compound at each sampling point. The time averaged uptake rates (*UR*, mL/min) based on the full 11-day experiment are shown for each chemical class on the plots to the right of Figure 3.

The parameters for the regression (power function) for the full 11-day sampling period and for the steady-state range of data (first 9-days) of sampling are provided in The calculated standard error of the estimate (*SEE*) is provided for the 11-day model to facilitate uncertainty estimates of the uptake rates. The two models do not differ significantly at the 9-day sampling duration (slope = 1.06) as shown in Figure 4. The largest difference for the predictions are for the compounds at the extremes of the physiochemical property range where the prediction for n-pentane (high volatility, low lipophilicity) was 12% higher for the steady-state range while several alkoxy compounds (low volatility, high lipophilicity) had higher uptake rates that were 12% − 16% higher when predicted from the full data range. This demonstrates the importance of sorbent selection for specific compounds. The Tenax-TA is a good sorbent for a wide range of compounds but may not be strong enough for compounds with high volatility and low lipophilicity.
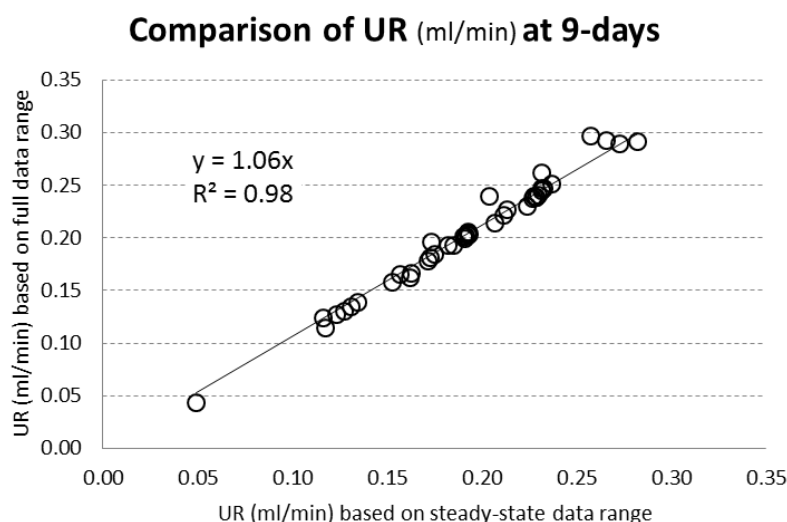
Figure 4. Comparison of the predicted uptake rates at nine days using the regressions parameterized using either the steady-state range of data (x-axis) or the full 11-day data range (y-axis). The model parameters for the power function are provided in Table 1 and used to calculate the UR (mL/min) for a 9-day sampling period.

Uptake rate determined for terpene on Tenax-GR without diffusion caps

In addition to the formal uptake experiment described above, uptake rates were determined during the loading phase of the ozone experiment. The same method was used to expose the tubes with VOCs for ozone testing and for determination of uptake rates in the previous section except that only terpenes were included in the ozone experiment. Tubes used in the ozone experiment did not have diffusion caps installed during uptake and the tubes contained Tenax-GR rather than Tenax-TA as the sorbent. Tenax-GR is a composite material that contains 30% graphite with Tenax which is expected to increase the capacity of the sorbent. Compared to Tenax-TA, Tenax-GR has a slightly lower specific surface area (24.1 m^2/g versus 30 m^2/g) and higher density (55 g/mL versus 25 g/mL). Uptake rates for the five terpenes used in the experiment were determined during the seven-day loading period for comparison to the Tenax-TA with diffusion caps installed.

The difference for uptake rates of the terpenes determined with and without the diffusion cap as a function of time is shown in Figure 5. As expected, the diffusion cap reduces the uptake rate because of a slight increase in the diffusion path length and a reduction in the cross sectional area of the tube inlet caused by the cap and screen. The average uptake rate over the sampling period from day 5 to through day 7 for the five terpenes is about 22% lower with the diffusion cap installed compared to without the diffusion caps. We focus on days 5 − 7 because tubes collected earlier in the sampling period have are more variable due to low sample mass. The difference between the tubes with diffusion caps and those without caps corresponds to an average uptake rate (±standard error) for the five terpenes of 0.258 ± 0.007 mL/min and 0.206 ± 0.005 mL/min for the uncapped tubes and capped tubes, respectively. Although the study was not designed to compare uptake rates for different sorbents, initial findings show that Tenax-GR tubes have a higher capacity (longer linear uptake phase) compared to the Tenax-TA tubes.

Ozone effect

After loading the diffusive sampling tubes with the five terpenes for seven days, the remaining twelve tubes were separated into four treatments as follows.

- No ozone: uncapped tubes installed in an ozone free chamber supplied with house air that had been conditioned through activated carbon and a HEPA filter running at approximately 2 air changes per hour
- Ozone positive control: uncapped tubes installed in the CSTR running with elevated ozone
- Ozone denuder: tubes with section of untreated denuder installed on the inlet simulating the change in axial diffusive tube geometry without ozone scrubbing
- Ozone KI denuder: tubes with section of potassium iodide treated denuder installed on the inlet to prevent ozone from reaching the sorbed terpenes.

In addition to the four treatments, we include results from the final sampling point of the uptake experiment as a starting mass (*initial*, ng) on the tubes. At the end of the treatments, all tubes were harvested and analysed and the average mass (ng, ± standard error) on tubes from each treatment are shown in Figure 6.

Figure 5. Influence of the diffusion cap on the uptake rate as a function of elapsed time for terpenes where percent difference is calculated as $(UR_o-UR_c)/average(UR_o, UR_c)$. UR_o is the uptake rate determined with axial-diffusion tube end open and UR_c is the uptake rate determined with a diffusion cap installed during uptake. The average for all terpenes and tubes over days five through seven indicates a 22% reduction in uptake rate with caps installed. Measurements collected earlier in the experiment show more variability while the uptake rate converges for most of the compound by day 7. It is unknown why the diffusion cap effect is greater for g-terpinene.

Table 1 and can be used to calculate sample volume (or uptake rate) as a function of sampling time for Tenax-TA axial diffusion tubes with diffusion caps under typical indoor conditions using Equation 7.
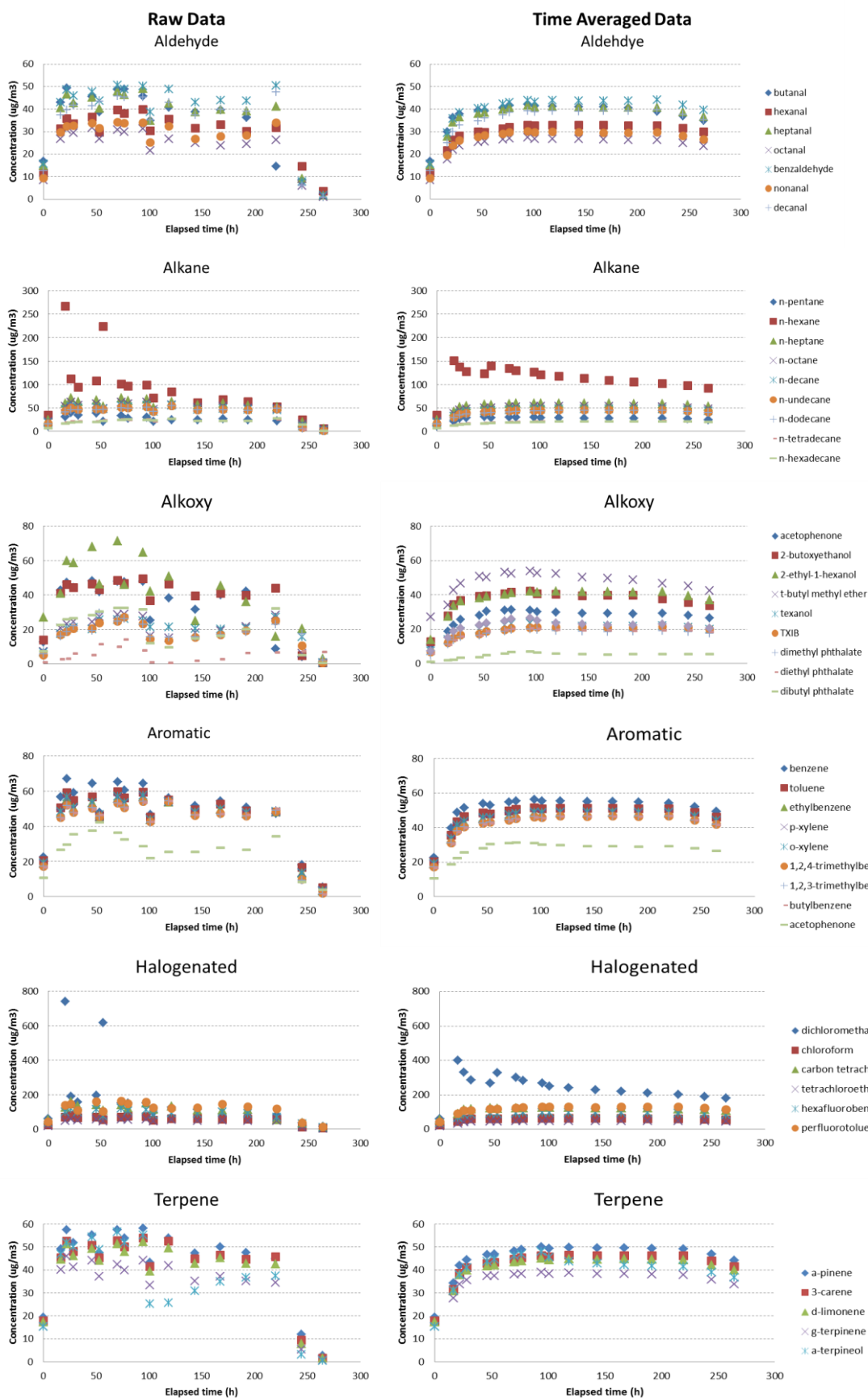
Figure 2: Concentration trend lines for each chemical class plotted over the uptake experiment with raw data plotted in the left column and time averaged or integrated concentrations plotted in the right column.
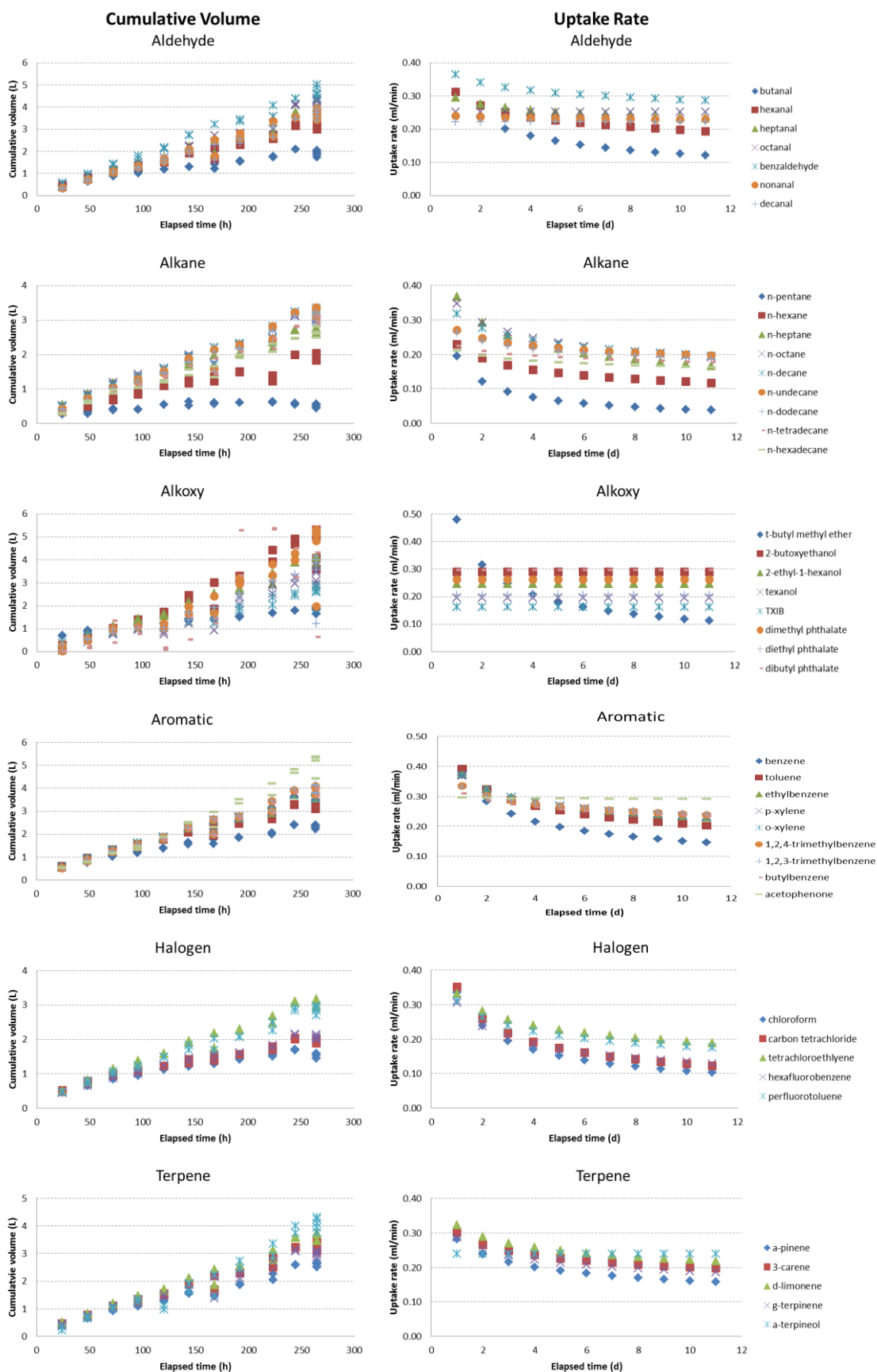
Figure 3. Trend of cumulative volume sampled for each compound in the left column and time averaged uptake rate in the right column.

The calculated standard error of the estimate (*SEE*) is provided for the 11-day model to facilitate uncertainty estimates of the uptake rates. The two models do not differ significantly at the 9-day sampling duration (slope = 1.06) as shown in Figure 4. The largest difference for the predictions are for the compounds at the extremes of the physiochemical property range where the prediction for n-pentane (high volatility, low lipophilicity) was 12% higher for the steady-state range while several alkoxy compounds (low volatility, high lipophilicity) had higher uptake rates that were 12% − 16% higher when predicted from the full data range. This demonstrates the importance of sorbent selection for specific compounds. The Tenax-TA is a good sorbent for a wide range of compounds but may not be strong enough for compounds with high volatility and low lipophilicity.

Comparison of UR (ml/min) **at 9-days**

Figure 4. Comparison of the predicted uptake rates at nine days using the regressions parameterized using either the steady-state range of data (x-axis) or the full 11-day data range (y-axis). The model parameters for the power function are provided in Table 1 and used to calculate the UR (mL/min) for a 9-day sampling period.

Uptake rate determined for terpene on Tenax-GR without diffusion caps

In addition to the formal uptake experiment described above, uptake rates were determined during the loading phase of the ozone experiment. The same method was used to expose the tubes with VOCs for ozone testing and for determination of uptake rates in the previous section except that only terpenes were included in the ozone experiment. Tubes used in the ozone experiment did not have diffusion caps installed during uptake and the tubes contained Tenax-GR rather than Tenax-TA as the sorbent. Tenax-GR is a composite material that contains 30% graphite with Tenax which is expected to increase the capacity of the sorbent. Compared to Tenax-TA, Tenax-GR has a slightly lower specific surface area (24.1 m^2/g versus 30 m^2/g) and higher density (55 g/mL versus 25 g/mL). Uptake rates for the five terpenes used in the experiment were determined during the seven-day loading period for comparison to the Tenax-TA with diffusion caps installed.

The difference for uptake rates of the terpenes determined with and without the diffusion cap as a function of time is shown in Figure 5. As expected, the diffusion cap reduces the uptake rate because of a slight increase in the diffusion path length and a reduction in the cross sectional area of the tube inlet caused by the cap and screen. The average uptake rate over the sampling period from day 5 to through day 7 for the five terpenes is about 22% lower with the diffusion cap installed compared to without the diffusion caps. We focus on days 5 − 7

16

because tubes collected earlier in the sampling period have are more variable due to low sample mass. The difference between the tubes with diffusion caps and those without caps corresponds to an average uptake rate (±standard error) for the five terpenes of 0.258 ± 0.007 mL/min and 0.206 ± 0.005 mL/min for the uncapped tubes and capped tubes, respectively. Although the study was not designed to compare uptake rates for different sorbents, initial findings show that Tenax-GR tubes have a higher capacity (longer linear uptake phase) compared to the Tenax-TA tubes.

Ozone effect

After loading the diffusive sampling tubes with the five terpenes for seven days, the remaining twelve tubes were separated into four treatments as follows.

- No ozone: uncapped tubes installed in an ozone free chamber supplied with house air that had been conditioned through activated carbon and a HEPA filter running at approximately 2 air changes per hour
- Ozone positive control: uncapped tubes installed in the CSTR running with elevated ozone
- Ozone denuder: tubes with section of untreated denuder installed on the inlet simulating the change in axial diffusive tube geometry without ozone scrubbing
- Ozone KI denuder: tubes with section of potassium iodide treated denuder installed on the inlet to prevent ozone from reaching the sorbed terpenes.

In addition to the four treatments, we include results from the final sampling point of the uptake experiment as a starting mass (*initial*, ng) on the tubes. At the end of the treatments, all tubes were harvested and analysed and the average mass (ng, ± standard error) on tubes from each treatment are shown in Figure 6.

Figure 5. Influence of the diffusion cap on the uptake rate as a function of elapsed time for terpenes where percent difference is calculated as $(UR_o - UR_c)/\text{average}(UR_o, UR_c)$. UR_o is the uptake rate determined with axial-diffusion tube end open and UR_c is the uptake rate determined with a diffusion cap installed during uptake. The average for all terpenes and tubes over days five through seven indicates a 22% reduction in uptake rate with caps installed. Measurements collected earlier in the experiment show more variability while the uptake rate converges for most of the compound by day 7. It is unknown why the diffusion cap effect is greater for g-terpinene.

17

Table 1. Parameters for estimating diffusive sample volume[1] as a function of time ($V = M*t^Z$)

Compound	11-day sampling period				9-day sampling period		
	z	m	r^2	*SEE*	z	m	r^2
butanal	0.609	0.064	0.98	0.06	0.589	0.070	0.98
hexanal	0.803	0.035	0.99	0.12	0.766	0.041	0.98
heptanal	0.902	0.024	0.99	0.18	0.868	0.028	0.99
octanal	0.999	0.015	0.98	0.32	0.951	0.019	0.98
benzaldehyde	0.898	0.030	0.99	0.22	0.871	0.034	0.99
nonanal	0.979	0.015	0.99	0.19	0.958	0.017	0.98
decanal	0.999	0.013	0.98	0.21	0.961	0.016	0.98
n-pentane	0.317	0.102	0.74	0.03	0.419	0.067	0.92
n-hexane	0.721	0.033	0.97	0.09	0.669	0.041	0.97
n-heptane	0.671	0.063	0.99	0.06	0.640	0.071	0.99
n-octane	0.753	0.046	0.99	0.11	0.714	0.054	0.99
n-decane	0.797	0.036	0.98	0.14	0.758	0.043	0.99
n-undecane	0.866	0.025	0.98	0.15	0.820	0.030	0.98
n-dodecane	0.858	0.025	0.98	0.15	0.815	0.030	0.98
n-tetradecane	0.904	0.018	0.99	0.10	0.865	0.021	0.99
n-hexadecane	0.892	0.018	0.98	0.07	0.874	0.019	0.98
benzene	0.611	0.077	0.99	0.03	0.587	0.084	0.99
toluene	0.723	0.057	0.99	0.08	0.698	0.063	0.99
ethylbenzene	0.795	0.043	0.99	0.14	0.762	0.049	0.99
p-xylene	0.808	0.041	0.99	0.16	0.772	0.047	0.99
o-xylene	0.797	0.042	0.99	0.15	0.760	0.049	0.99
1,2,4-trimethylbenzene	0.858	0.031	0.99	0.21	0.813	0.038	0.99
1,2,3-trimethylbenzene	0.865	0.031	0.98	0.22	0.818	0.037	0.99
butylbenzene	0.884	0.027	0.99	0.20	0.842	0.032	0.99
acetophenone	0.995	0.018	0.97	0.65	0.918	0.025	0.97
2-butoxyethanol	1[2]	0.017	0.98	1.13	1	0.016	0.98
2-ethyl-1-hexanol	1	0.015	0.99	0.21	0.963	0.017	0.99
t-butyl methyl ether	0.395	0.197	0.98	0.02	0.374	0.215	0.99
texanol	1	0.012	0.97	0.67	1	0.010	0.95
TXIB	1	0.010	0.98	0.25	1	0.010	0.98
dimethyl phthalate	1	0.016	0.94	2.60	1	0.014	0.96
diethyl phthalate	1	0.012	0.94	1.57	1	0.012	0.97
dibutyl phthalate	1	0.018	0.78	15.25	1	0.015	0.75
chloroform	0.509	0.096	0.98	0.03	0.535	0.086	0.99
carbon tetrachloride	0.562	0.085	0.99	0.02	0.541	0.092	0.99
tetrachloroethlyene	0.767	0.042	0.99	0.09	0.736	0.047	0.99
hexafluorobenzene	0.642	0.057	0.99	0.03	0.615	0.064	0.99
perfluorotoluene	0.761	0.040	0.99	0.08	0.723	0.047	0.99
a-pinene	0.757	0.037	0.99	0.07	0.716	0.043	0.99
3-carene	0.825	0.031	0.98	0.14	0.779	0.038	0.99
d-limonene	0.838	0.033	0.98	0.18	0.791	0.039	0.98
g-terpinene	0.820	0.030	0.97	0.18	0.786	0.035	0.96
a-terpineol	1	0.014	0.93	0.67	0.985	0.013	0.93

[1]Parameters are for sample volume in Liters as a function of time in days; [2] when the best fit exponenet is greater than one, $z > 1$, the exponent is set to 1 and the model reduces to a linear regression with slope (m).
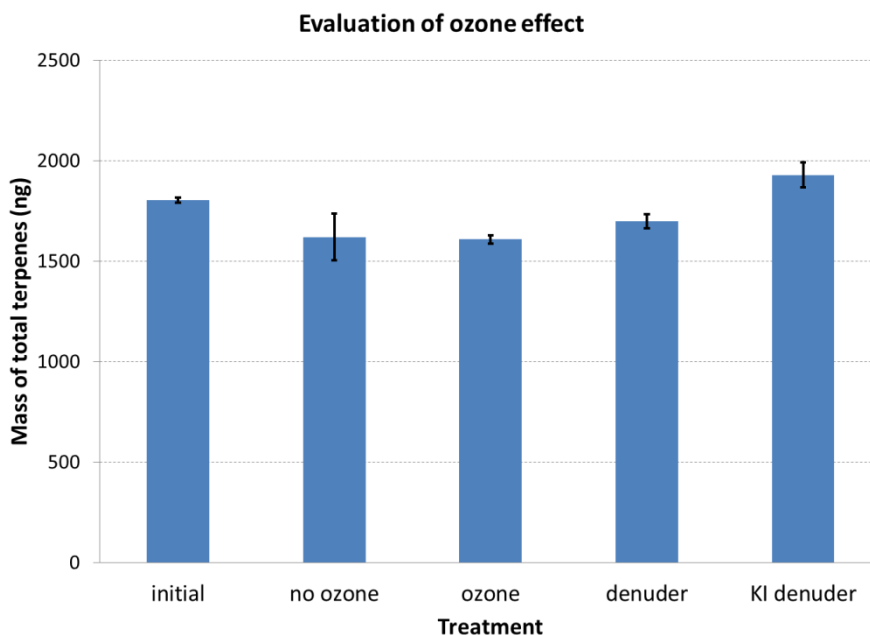
Figure 6. Effect of different ozone exposure scenarios on total terpene mass (sum of five terpenes) on passively loaded tubes where error bars indicate ± 1 standard error.

DISCUSSION

The shape of the uptake curve for diffusive sampling should be linear, i.e., a constant uptake rate, over the duration of the sampling event so that the resulting measurements represent a time averaged concentration. If sampling is faster or slower during part of the sampling period, the measurement will be biased in favour of the period where sampling rate was elevated. Many of the compounds included in this work had initial uptake rates that were faster than the long-term average sampling rate and the shape of the curve in terms of cumulative volume sampled over time was best described using a power function. The power function has a zero intercept and approaches a straight line (when the uptake rate is constant over time) as the value of the exponent of the power function approaches one.

The relationship between the two parameters of the power function (Equation 7) for the VOCs tested in this work is shown in Figure 7 where the value of the constant (m) was plotted against the value of the corresponding exponent (z) across all compounds in this study. The two outliers in the relationship are compounds with both high vapour pressure and low sorbent capacity, a combination that may be outside the useable range of the Tenax-TA axial-diffusion sampling tubes. The parameterized second order polynomial shown in Figure 7 does not change significantly if the outliers – pentane and methyl tert-butyl ether (mtbe) – are excluded from the regression. We use the relationship between the parameter pairs (z, m) for the actual compounds to simulate a set of uptake curves to further explore the performance of the passive samplers.

The equation shown in Figure 7 was used to generate a set of parameter pairs (z, m) that represent the range of compounds in this study. The parameter pairs were used with Eq 7 to construct representative curves of cumulative sample volume as a function of time shown in Figure 8. These curves illustrate how the deviation from a linear or constant uptake rate is related to the value of z and the long-term uptake rate is controlled by the value of m. When z is small, the uptake rate is initially fast but slows with time and as z approaches unity the

19

uptake rate becomes linear (constant). Increasing the value of *m* with no change to *z* results in an increase in the long-term uptake rate (slope).
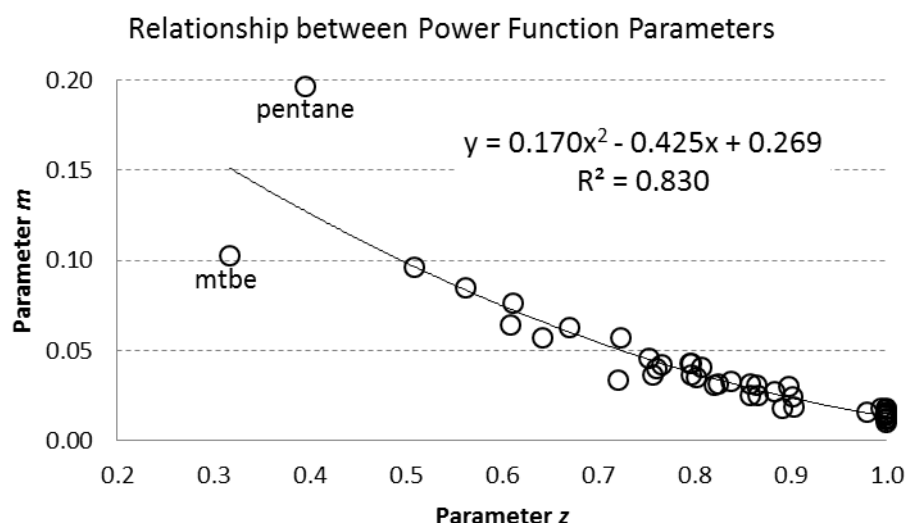
Figure 7. Relationship between the power function constant (*m*) and the exponent (*z*) for the test compounds. The coefficient of determination (r^2) of the regression increases to 0.95 when pentane and methyl tert-butyl ether (MTBE) are excluded without changing the model. The polynomial regression is used to construct representative parameter pairs (*z, m*) across the range of VOCs to explore the shape of the uptake curves for the compounds in Table 1.
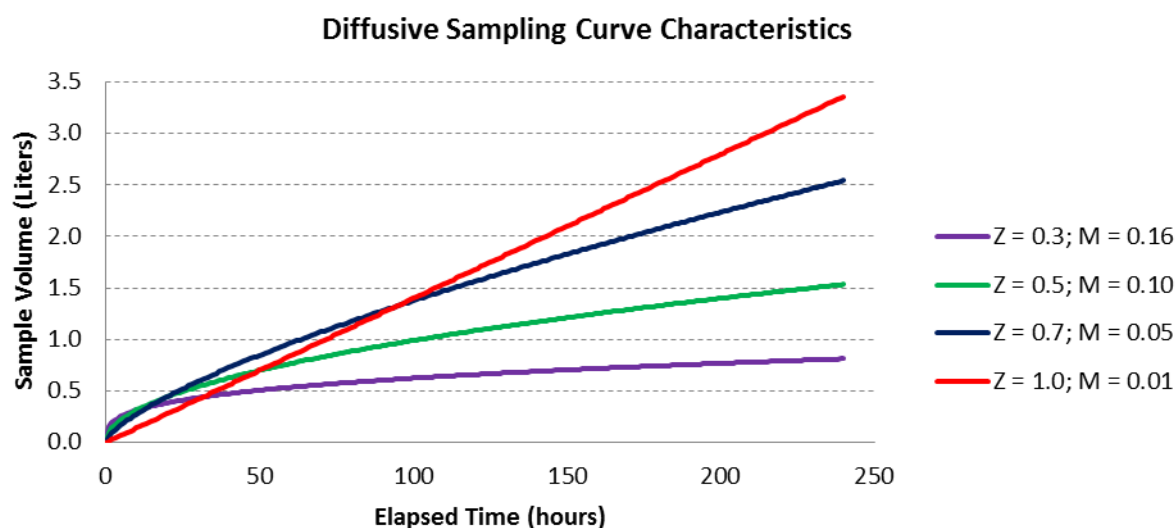
Figure 8. Set of illustrative curves showing the shape of the sample volume (V, L) to elapsed time (h) relationship for representative parameter pairs that were generated using the regression shown in Figure 7. The straight line indicates a constant uptake rate while the curved lines indicated initial rapid uptake followed by slower long term uptake.

Although the values of the parameters in the power function describe the shape of the uptake rate curve, the reason for the difference in the shape of the curve is related to physiochemical properties of the VOCs. Assuming constant sampler geometry, the two properties that

20

influence the uptake rate are the molecular diffusivity and the sorbent/air partition coefficient. This is illustrated in Figure 9 along with a cross-section schematic of an axial-diffusive sampling tube.

Referring to Figure 9, when the tube is opened and sampling starts, the concentration at the sorbent/air interface is effectively zero and uptake is controlled by the molecular diffusivity of the compound in air following Fick's Law (Equation 1). The resulting concentration profile across the length of the sampling tube is illustrated for this case in the upper chart in Figure 9 below the schematic of the sampling tube. The concentration gradient at the inlet to the sampling tube goes from the ambient air concentration at the open face of the diffusion cap to effectively zero on the air-side of the sorbent/air interface.

As sampling progresses, the concentration on the sorbent-side of the sorbent/air interface begins to increase but the effective concentration on the air-side of the sorbent/air interface remains near zero so that the uptake is still controlled only by molecular diffusion. This case is illustrated by the second chart shown in Figure 8. As the concentration on the sorbent-side of the sorbent/air interface increases, th e chemical begins to diffuse into the sorbent bed. The rate of diffusion into the sorbent bed is controlled by the effective diffusivity of the compound in the sorbent which is a function of the molecular diffusivity of the compound and the porosity of the sorbent bed. When air occupies a tortuous pathway between stationary particles in a porous medium, Millington and Quirk (1961) have shown that the effective diffusivity, D_{eff}, of a chemical in the fluid-filled pore space is given by

$$D_{eff} = \frac{\varepsilon^{10/3}}{\phi^2} D_{pure} \tag{11}$$

where ε is the volume fraction occupied by the fluid, ϕ is the total void fraction in the medium (the volume occupied by all fluids), and D_{pure} is the molecular diffusivity or diffusion coefficient of the chemical in the pure fluid. Given a completely dry sorbent bed of Tenax-TA with pore space of 0.6, the effective diffusivity in the sorbent bed is about ½ the molecular diffusivity in air.

At some point in time after sampling begins, the concentration on the sorbent side of the sorbent/air interface reaches a level above which the air-side concentration is no longer zero. This is illustrated in the bottom graphic in Figure 9. This is the point where the sorbent-side concentration divided by the air-side concentration equals the equilibrium sorbent/air partition coefficient. As diffusive sampling continues beyond this point, the concentration on each side of the sorbent/air interface will continue to increase resulting in a downward trend in the sampling rate. The downward trend in sampling rate is caused by a decrease in the concentration gradient between the ambient air concentration at the entrance to the sorbent tube and the concentration on the air-side of the sorbent/air interface.

The sorbent-side and air-side concentration will continue to increase and the sampling rate will continue to decrease until the uptake rate is controlled by the effective diffusivity in the sorbent bed. Once sampling rate from air is equal to the diffusion rate into the sorbent bed, the concentration at the sorbent/air interface will stop increasing and sampling will be constant again, controlled only by the effective diffusivity.

Diffusion path length   Porous sorbent bed

Tube opening

Diffusion cap & screen

C_{air}

sorbent/air interface

Increasing Conc. in Air

C^*_{air} $C^*_{sorbent}$

Increasing Conc. in Sorbent

Time = t_0 = start

$c^*_{air} = c^*_{sorbent} = 0$

C_{air}

Increasing Conc. in Air

$C^*_{sorbent}$

C^*_{air}

Increasing Conc. in Sorbent

Time = $t_{(n)} = t_0 + \Delta t$

$c^*_{air} = 0$

$c^*_{sorbent} > 0$

C_{air}

$C^*_{sorbent}$

Increasing Conc. in Air

C^*_{air}

Increasing Conc. in Sorbent

Time = $t_{(n+1)} = t_{(n)} + \Delta t$

$c^*_{air} \sim 0$

$\dfrac{c^*_{sorbent}}{c^*_{air}} = K_{(sorbent/air)}$

Increasing distance into tube

Figure 9. Schematic of axial-diffusion sampling tube is shown in the top image. The three graphics below the schematic illustrate the concentration profile as a function of time. The top graphic illustrates the concentration profile shortly after the start of a sampling event and the subsequent graphics illustrate the change in concentration profile as sampling progresses. The symbols are as follows – C_{air} is the ambient concentration of the target chemical in air; C^*_{air} is the air concentration directly adjacent to the air/sorbent interface; $C^*_{sorbent}$ is the concentration in the sorbent directly adjacent to the air/sorbent interface; and $K_{(sorbent/air)}$ is the equilibrium partition coefficient between sorbent and air.

The time that it takes for the sampling to move through the different stages described above is also a function of the physiochemical properties. Increasing molecular diffusivity and/or decreasing the sorbent/air partition coefficient will shorten the time required to go from the air-side diffusion controlled uptake to the transition between air-side and sorbent-side diffusion controlled uptake and then finally to sorbent-side diffusion controlled uptake.

Walgraeve et.al. (2011a) defined the term "sampling efficiency (*SE*)" as the ratio of the experimental uptake rate to the theoretical or ideal uptake rate and found that the sorbent/air partition coefficient explained much of the deviation of uptake rates from the ideal. Using the octanol/air partition coefficient (K_{oa})as a surrogate for the sorbent/air partition coefficient in this work we see a similar pattern in *SE* as was shown by Walgraeve et.al., (2011a). Figure 10 shows *SE* increasing with sorption capacity up to a Log K_{oa} of about 4.5. Beyond a Log K_{oa} of 4.5, the *SE* is relatively insensitive to the sorbent/air partition coefficient remaining constant at about 0.78.
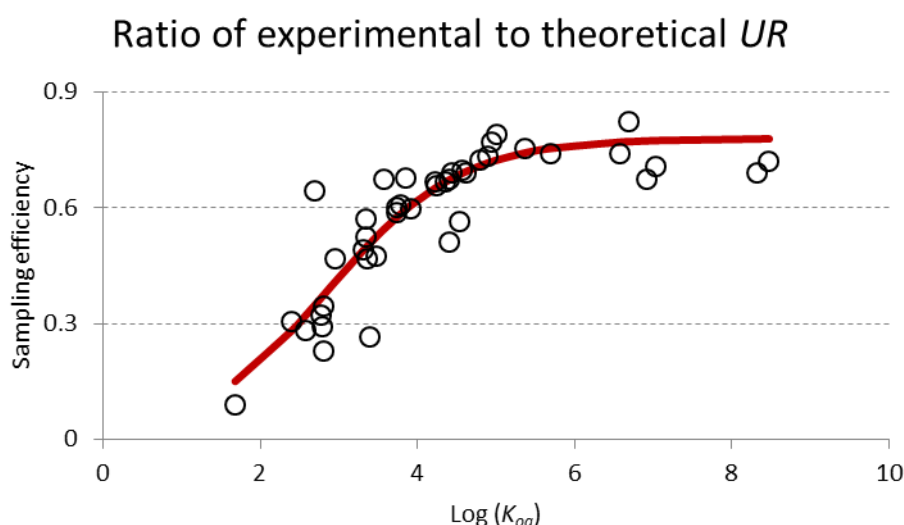
Figure 10. Sampling efficiency calculated as the ratio of the time averaged experimental uptake at 11-days to the theoretical uptake rate based on molecular diffusivity and tube geometry. The line through the data is an off-set logistic function fit by minimizing the sum of the squares between the experimental and predicted values.

The constant *SE* above Log K_{oa} of 4.5 indicates that the sorption capacity of the sorbent interface has not been exceeded for the conditions of sampling resulting in near ideal uptake. The ~ 20% reduction in sampling rate observed with the experimental uptake rates relative to ideal value calculated from molecular diffusivity and tube geometry may be due to the diffusion caps as illustrated in Figure 5 earlier. The experiment with terpenes indicated that having diffusion caps installed during sampling reduced uptake rates by approximately 20% over a 7-day sampling period. This may be due to a reduction in the opening caused by the wire gauze and clip and/or an increase in diffusion path caused by the cap.

The line fit through the *SE* data in Figure 10 is a logistic function of the form

$$SE = \frac{SE_{max}}{1+\left(\frac{1}{A}-1\right)e^{-B\times(LogKoa-offset)}} \tag{12}$$

Where SE_{max} is the maximum ratio of the experimental to theoretical sampling rates, A and B are constants and *offset* shifts the curve along the sorbent/air partition coefficient axis. The value of the *offset* is likely related to the sorbent being used where a stronger sorbent (i.e., graphitized carbon) would reduce the *offset* such that chemicals with lower Log K_{oa} would approach the SE_{max}. The parameters in the model were adjusted to minimize the sum of the square differences between the experimental and predicted sampling efficiency values. Equation 12 can be used to predict SE for chemicals that lack experimentally determined uptake rate given the conditions of this study using the chemical's Log Koa and parameter values for *A, B* and *offset* of 0.26, 1.2 and 2, respectively. The standard error of the estimate for Equation 12 is 0.089 in the Log K_{oa} range of 1.7 to 8.5. The predicted SE can then be used with the theoretical uptake rate (Equation 1) to predict the time-averaged uptake rate for the chemical at 11-days.

The ozone experiment produced an additional set of uptake curves for terpenes in the absence of diffusion caps. The uptake rates were approximately 20% faster at 7 days compared to those determined with diffusion caps installed. These differences should be explored further to confirm the changes in tube geometry related to the use of the diffusion caps and improve the estimate of the theoretical uptake rate. The results indicate that the wire gauze and cap reduce the cross-sectional area of the tube opening and/or increase the diffusion path length but it is important to use the diffusion caps to reduce effects of variable wind speed on sampling rate (Pennequin-Cardinal et.al., 2005).

The results for the different ozone treatments were compared statistically using the Student's t-test with results shown in Table 2. The comparison shows that the only statistically significant difference in the treatments is between the "no ozone" treatment (no denuder) and the "with ozone" treatment using the KI coated denuder (p-value 0.01), and between the "with ozone" treatment for KI coated denuder and uncoated denuder (p-value 0.03). However, neither treatment is significantly different from the initial concentration. In addition, the treatments using denuders are actually slightly higher than the initial mass on the tubes measured at the start of the ozone exposure.

Table 2. Student's t-test probability matrix comparing different treatments

			with ozone		
		no ozone	without denuder	with uncoated denuder	with KI coated denuder
	no ozone	1.00	0.93	0.55	0.08
with ozone	without denuder		1.00	0.09	**0.01**
with ozone	with uncoated denuder			1.00	**0.03**
with ozone	with KI coated denuder				1.00

The important comparison for understanding possible ozone degradation of the sorbed terpenes is between the "no ozone" treatment without denuder and the "with ozone" treatment without denuder. These treatments had exactly the same tube geometry with the only difference in the treatments being the presence/absence of ozone. In this comparison, the final mass of total terpene for the two treatments was not significantly different. There was no apparent influence of ozone on terpene loss. Possible reasons slightly higher mass on the tubes with denuders may be random error or may be related to back diffusion of sorbed chemical. The rate of back diffusion would be different for the tubes using denuders and those without denuders because of difference in the diffusion path length of the additional section of

denuder tube and reduce in diffusion cross sectional area because of the coating on the walls of some of the denuders.

CONCLUSION

Diffusive sampling using commercial thermal desorption tubes is a reliable method for monitoring air contaminants over long sampling periods. Compared to active sampling methods, passive sampling is cost effective and easy to deploy by untrained personnel. The Tenax-TA axial-diffusive sampling tubes are appropriate for chemicals ranging in vapour pressure and lipophilicity from n-pentane to dibutyl phthalate as shown in this work.

The CSTR calibration chamber and VOC delivery system used in this study provides field relevant uptake rates for a wide range of relevant indoor pollutants. Compounds at the extreme high end of the volatility range and low end of the lipophilicity range (e.g., n-pentane, butanal and n-hexane) have faster uptake rates early in the sampling period relative to the long term average uptake rate leading to a possible bias in the measured concentrations towards the early period of deployment. Uncertainty in the experimental sampling rates increases for compounds with very high lipophilicity and low vapour pressure (e.g., phthalates). Most of the compounds tested had excellent precision. Five tubes were collected at the 11-day sampling point and the measured uptake rates for all compounds except 2-butoxyethanol and dibutyl phthalate had coefficient of variation better than 10% with more than 70% of the compounds having precision better than 4.7%. Therefore, even if the uptake was not always constant for different sample durations, the sampling rate at any given sample duration was highly reproducible.

For chemicals that are listed in Table 1, we recommend using the power function parameters (*m* and *z*) derived from the 11-day sampling period to estimate cumulative sample volume for sample durations between one and 11 days. The standard error of the estimate is provided for each compound for reporting uncertainty in the estimated sampling rate. For compounds not listed in Table 1, but with physiochemical properties in the range of the tested compounds (see Appendix 1) we recommend using Equation 12 for the logistic function that is illustrated in Figure 10. The standard error of the estimate is provided with Equation 12 for reporting uncertainty. The predicted *SE* can then be used with the theoretical uptake rate (Equation 1) to estimate the appropriate uptake rate. It is important to note that the predicted *SE* is for diffusive sampling over the full 11-days while the parameters in Table 1 can be used for shorter sampling periods but only within the test range (1 to 11 days).

Future work should confirm the influence of diffusion caps on the theoretical uptake rate calculated from molecular diffusivity and tube geometry so that a more reliable estimate of the theoretical uptake rate can be made. In addition, different sorbents and commercial tubes should be tested to further refine the parameters in Equation 12, which may lead to a generalizable predictive equation for uptake based on sorbent type, tube geometry and physiochemical properties. It would also be useful to confirm the temperature and pressure relationship in Equation 5 although indoor sampling is typically conducted near standard temperature and pressure.

REFERENCES

Brown, J., & Shirey, B. (2001). A tool for selecting an adsorbent for thermal desorption applications. Supelco, Inc., Bellefonte, PA, Tech. Rep. T, 402025, 2001. http://www.sigmaaldrich.com/analytical-chromatography/air-monitoring/learning-center/td-tube-selector.html (checked February 25, 2013)

Calogirou, A., Larsen, B. R., Brussol, C., Duane, M., & Kotzias, D. (1996). Decomposition of terpenes by ozone during sampling on Tenax. *Analytical Chemistry*, 68(9), 1499-1506.

Coleman, B. K., Lunden, M. M., Destaillats, H., & Nazaroff, W. W. (2008). Secondary organic aerosol from ozone-initiated reactions with terpene-rich household products. *Atmospheric Environment*, 42(35), 8234-8245.

Gonzalez-Flesca, N., & Frezier, A. (2005). A new laboratory test chamber for the determination of diffusive sampler uptake rates. *Atmospheric Environment*, 39(22), 4049-4056.

Heck, W. W., Philbeck, R. B., & Dunning, J. A. (1978). A continuous stirred tank reactor (CSTR) system for exposing plants to gaseous air contaminants. Principles, specificatiions, construction, and operation [Air pollution injuries, beans]. ARS-S-US Agricultural Research Service.

Hodgson A.T. and H. Levin (2003) "Volatile organic compounds in indoor air: A review of the concentrations measured in North America since 1990" LBNL-51715. Lawrence Berkeley National Laboratory.

Jeffries, H. E., Rogers, H. H., & Stahel, E. P. (1976). Spatially uniform environment for the dynamic study of biological sys-tems: application of the continuous stirred tank reactor concept. *Sci. Biol. J*, 2, 180-182.

Jia, C., Batterman, S. A., & Relyea, G. E. (2012). Variability of indoor and outdoor VOC measurements: An analysis using variance components. *Environmental Pollution*. 169. 152-159

Kleindienst, T. E., Corse, E. W., Blanchard, F. T., & Lonneman, W. A. (1998). Evaluation of the Performance of DNPH-Coated Silica Gel and C18 Cartridges in the Measurement of Formaldehyde in the Presence and Absence of Ozone. *Environmental Science & Technology*, 32(1), 124-130.

Klepeis, N. E., Nelson, W. C., Ott, W. R., Robinson, J. P., Tsang, A. M., Switzer, P., Behar, J.V., Hern, S.C. and Engelmann, W. H. (2001). The National Human Activity Pattern Survey (NHAPS): a resource for assessing exposure to environmental pollutants. *Journal of exposure analysis and environmental epidemiology*, 11(3), 231-252.

Kumar, A., & Víden, I. (2007). Volatile organic compounds: Sampling methods and their worldwide profile in ambient air. *Environmental monitoring and assessment*, 131(1), 301-321.

Logue, J. M., McKone, T. E., Sherman, M. H., & Singer, B. C. (2011). Hazard assessment of chemical air contaminants measured in residences. *Indoor air*, 21(2), 92-109.

Maddalena, R. L., McKone, T. E., & Kado, N. Y. (2002). Exposure chamber measurements of mass transfer and partitioning at the plant/air interface. *Environmental science & technology*, 36(16), 3577-3585.

Maddalena, R., N. Li, A. Hodgson, F. Offermann and B. Singer (2012) "Maximizing Information from Residential Measurements of Volatile Organic Compounds". Health Buildings 2012 Conference Proceedings. LBNL-Pending. Lawrence Berkeley National Laboratory

Pennequin-Cardinal, A., Plaisance, H., Locoge, N., Ramalho, O., Kirchner, S., & Galloo, J. C. (2005). Dependence on sampling rates of Radiello® diffusion sampler for BTEX measurements with the concentration level and exposure time. *Talanta*, 65(5), 1233-1240.

Pollmann, J., Ortega, J., & Helmig, D. (2005). Analysis of atmospheric sesquiterpenes: Sampling losses and mitigation of ozone interferences. *Environmental science & technology*, 39(24), 9620-9629.

Rogers, H. H., Jeffries, H. E., Stahel, E. P., Heck, W. W., Ripperton, L. A., & Witherspoon, A. M. (1977). Measuring air pollutant uptake by plants: a direct kinetic technique. *Journal of the Air Pollution Control Association*, 27(12), 1192-1197.

Satish, U., Fisk, W. B., Mendell, M. J., Eliseeva, K., Hotchi, T., Sullivan, D., ... & Teng, K. (2011). Impact of CO2 on human decision making and productivity. *Journal of Applied Social Psychology*, 23, 847-866.

Springs, M., Wells, J. R., & Morrison, G. C. (2011). Reaction rates of ozone and terpenes adsorbed to model indoor surfaces. *Indoor Air*, 21(4), 319-327.

Tucker, W. A., & Nelken, L. H. (1990). Diffusion coefficients in air and water. IN: Handbook of Chemical Property Estimation Methods: Environmental Behavior of Organic Compounds. American Chemical Society, Washington, DC. 1990. p 17. 1-17. 25. 7 tab, 28 ref.

Walgraeve, C., Demeestere, K., Dewulf, J., Van Huffel, K., & Van Langenhove, H. (2011a). Diffusive sampling of 25 volatile organic compounds in indoor air: Uptake rate determination and application in Flemish homes for the elderly. *Atmospheric Environment*, 45(32), 5828-5836.

Walgraeve, C., Demeestere, K., Dewulf, J., Van Huffel, K., & Van Langenhove, H. (2011b). Uptake rate behavior of tube-type passive samplers for volatile organic compounds under controlled atmospheric conditions. *Atmospheric Environment*, 45(32), 5872-5879.

Woolfenden, E. A., & McClenny, W. A. (1999). Compendium Method TO-17. Determination of volatile organic compounds in ambient air using active sampling onto sorbent tubes. Compendium Methods for the Determination of Toxic Organic Compounds in Ambient Air, 2te Auflage,(Ed.: US Environmental Protection Agency), 1-53.

Yılmaz Civan, M., Yurdakul, S., & Tuncel, G. (2012). Improvement of uptake rate equations depending on meteorological conditions for 25 volatile organic compounds. *Talanta*. 99, 720-729

Appendix 1: List of Chemicals and Properties (see caption for definition of properties and units)[1]

Compound	Chemical Class	CAS#	MW	ρ	BP	V_x	H	Log K_{ow}	Log K_{oa}	D_{air}	CF
2-butoxyethanol	Alcohol	111-76-2	118.17	0.90	170	131.44	1.60E-06	0.83	5.01	0.073	0.207
2-ethyl-1-hexanol	Alcohol	104-76-7	130.23	0.83	185	158.47	2.65E-05	2.73	5.70	0.066	0.188
butanal	Aldehyde	123-72-8	72.10	0.80	75	91.88	1.15E-04	0.88	3.39	0.090	0.339
hexanal	Aldehyde	66-25-1	100.20	0.82	128	124.90	2.13E-04	1.78	4.41	0.076	0.244
heptanal	Aldehyde	111-71-7	114.20	0.82	153	141.40	2.70E-04	2.29	4.25	0.071	0.214
octanal	Aldehyde	124-13-0	128.20	0.82	174	157.91	5.14E-04	2.78	5.36	0.067	0.191
benzaldehyde	Aldehyde	100-52-7	106.10	1.05	179	101.10	2.67E-05	1.48	4.44	0.082	0.231
nonanal	Aldehyde	124-19-6	142.20	0.83	195	174.42	7.34E-04	3.27	4.79	0.063	0.172
decanal	Aldehyde	112-31-2	156.27	0.83	208	190.92	1.80E-03	3.76	4.89	0.060	0.157
n-pentane	Alkane	109-66-0	72.20	0.63	36	111.07	1.25E+00	3.39	1.68	0.083	0.339
n-hexane	Alkane	110-54-3	86.20	0.66	69	127.58	1.80E+00	3.90	2.40	0.076	0.284
n-heptane	Alkane	142-82-5	100.20	0.68	98	144.08	2.00E+00	4.66	2.95	0.071	0.244
n-octane	Alkane	111-65-9	114.20	0.70	126	160.59	3.21E+00	5.18	3.35	0.067	0.214
n-decane	Alkane	124-18-5	142.30	0.73	174	193.60	5.15E+00	5.01	2.69	0.060	0.172
n-undecane	Alkane	1120-21-4	156.30	0.74	196	210.11	1.93E+00	5.74	3.84	0.058	0.157
n-dodecane	Alkane	112-40-3	170.30	0.75	216	226.62	8.24E+00	6.10	3.57	0.055	0.144
n-tetradecane	Alkane	629-59-4	198.40	0.76	252	259.63	9.20E+00	7.20	4.63	0.051	0.123
n-hexadecane	Alkane	544-76-3	226.40	0.77	287	292.64	4.73E-01	8.20	6.91	0.048	0.108
benzene	Aromatic	71-43-2	78.11	0.87	80	89.43	5.55E-03	2.13	2.78	0.090	0.313
toluene	Aromatic	108-88-3	92.14	0.87	110	105.71	6.64E-03	2.73	3.31	0.082	0.266
ethylbenzene	Aromatic	100-41-4	106.17	0.87	136	122.25	7.88E-03	3.15	3.74	0.076	0.230
p-xylene	Aromatic	106-42-3	106.20	0.86	139	121.98	6.90E-03	3.15	3.79	0.076	0.230

Compound	Chemical Class	CAS#	MW	ρ	BP	V_x	H	Log K_{ow}	Log K_{oa}	D_{air}	CF
o-xylene	Aromatic	95-47-6	106.17	0.88	144	121.98	5.18E-03	3.12	3.91	0.076	0.230
1,2,4-trimethylbenzene	Aromatic	95-63-6	120.19	0.88	168	138.26	6.16E-03	3.63	4.23	0.071	0.204
1,2,3-trimethylbenzene	Aromatic	526-73-8	120.20	0.89	175	138.26	4.36E-03	3.66	4.41	0.071	0.204
butylbenzene	Aromatic	104-51-8	134.20	0.86	183	155.26	1.59E-02	4.38	4.57	0.067	0.182
acetophenone	Aromatic	98-82-2	120.15	1.03	202	120.96	1.04E-05	1.58	4.95	0.075	0.204
texanol	Ester	25265-77-4	216.32	0.95	255	228.78	4.23E-06	3.00	8.47	0.054	0.113
TXIB	Ester	6846-50-0	286.40	0.94	280	301.16	3.40E-03	4.91	8.32	0.047	0.085
dimethyl phthalate	Ester	131-11-3	194.18	1.19	282	165.22	1.97E-07	1.60	6.69	0.063	0.126
diethyl phthalate	Ester	84-66-2	222.20	1.12	298	198.23	6.10E-07	2.42	7.02	0.058	0.110
dibutyl phthalate	Ester	84-74-2	278.34	1.04	340	264.26	1.81E-06	4.50	8.63	0.050	0.088
t-butyl methyl ether	Ester	1634-04-4	88.20	0.74	20	117.48	5.87E-04	0.94	2.58	0.079	0.277
dichloromethane	Halogen	75-09-2	84.90	1.33	40	67.81	3.25E-03	1.25	2.27	0.100	0.288
chloroform	Halogen	67-66-3	119.40	1.49	62	79.57	3.67E-03	1.97	2.80	0.090	0.205
carbon tetrachloride	Halogen	56-23-5	153.80	1.59	77	90.63	2.76E-02	2.83	2.79	0.083	0.159
tetrachloroethlyene	Halogen	127-18-4	165.80	1.62	121	100.31	1.77E-02	3.40	3.48	0.079	0.148
hexafluorobenzene	Perfluorinated	392-56-3	186.05	1.61	81	114.69	2.68E+00	2.55	2.81	0.074	0.131
perfluorotoluene	Perfluorinated	434-45-7	236.06	1.66	104	143.99	8.16E-01	3.96	3.34	0.066	0.104
a-pinene	Terpene	7785-70-8	136.23	0.86	156	154.91	2.94E-01	4.48	3.36	0.067	0.180
3-carene	Terpene	13466-78-9	136.23	0.86	174	154.91	8.18E-02	4.38	3.74	0.067	0.180
d-limonene	Terpene	5989-27-5	136.23	0.84	175.5	163.26	3.19E-02	4.57	4.36	0.065	0.180
g-terpinene	Terpene	99-85-4	136.23	0.85	182	161.13	2.25E-02	4.50	4.54	0.066	0.180
a-terpineol	Terpene	10482-56-1	154.25	0.93	217	164.98	1.22E-05	3.28	6.58	0.064	0.159

[1] Properties listed in the header are defined as follows: CAS# is the chemical abstract service number; MW is molecular weight (g/mol); ρ is the liquid density at 20 °C (g/mL); BP is boiling point (°C), V_x is molar volume (cm^3/mol); H is Henry's law constant (atm-m^3/mol); Log K_{ow} is the log octanol water partition coefficient (unitless), Log K_{oa} is the octanol air partition coefficient (unitless), D_{air} is the molecular diffusivity in air (m^2/d); and CF is the conversion factor between µg/m^3 and ppb. MW and ρ were from the original container, BP, V_x, H, Log K_{ow} and Log K_{oa} were from http://www.chemspider.com/. D_{air} was calculated as described in the methods section.